Hindawi Publishing Corporation
Journal of Nanomaterials
Volume 2015, Article ID 907954, 8 pages
http://dx.doi.org/10.1155/2015/907954

Research Article

Fabrication and Properties of Macroscopic Carbon Nanotube Assemblies Transforming from Aligned Nanotubes

Y. N. Zhang,[1,2] G. Z. Sun,[2] and L. X. Zheng[2,3]

[1]*Science and Technology on Thermostructural Composite Materials Laboratory & State Key Laboratory of Solidification Processing, Northwestern Polytechnical University, Xi'an 710072, China*
[2]*School of Mechanical and Aerospace Engineering, Nanyang Technological University, Singapore 639798*
[3]*Department of Mechanical Engineering, Khalifa University, P.O. Box 127788, Abu Dhabi, UAE*

Correspondence should be addressed to Y. N. Zhang; yani-zhang@hotmail.com and G. Z. Sun; gzsunk@gmail.com

Received 30 November 2014; Revised 14 January 2015; Accepted 14 January 2015

Academic Editor: Hassan Karimi-Maleh

Macroscale assemblies of well-aligned carbon nanotubes (CNTs) can inherit intrinsic properties from individual CNTs and at the same time ease handling difficulties that occur at nanometer scale when dealing with individual CNTs. Herein, simple fabrication processes are introduced to produce a variety of macroscale CNT assemblies, including well-aligned CNT bundles, CNT films, and CNT fibers, from the same starting material: spinnable CNT arrays. The electrical and mechanical properties of the as-prepared CNT assemblies have been investigated and compared. It is found that CNT films show an electrical conductivity of 145~250 S cm^{-1} which is comparable to CNT fibers, but two orders magnitude higher than that of conventional Bucky paper. CNT fibers exhibit diameter dependent tensile strength which is mainly attributed to the nonuniform twisting along the radial direction of fibers.

1. Introduction

The excellent electrical, mechanical, thermal, and optical properties of one-dimensional (1D) carbon nanotubes (CNTs) provide them a wide range of potential applications [1–3]. In the past two decades, considerable attention has been paid to the use of CNTs as building blocks for high performance materials [4–7]. Due to their outstanding ballistic electronic conduction and insensitivity to electromigration, CNTs are able to withstand current densities up to 10^9 A cm^{-2}, which is a thousand times greater than that of noble metals [8]. Field effect transistors (FETs) [9, 10] and even logic circuits [11, 12] from individual CNTs have been demonstrated due to their high charge mobility (up to 10 000 cm^2 V^{-1} s^{-1}). Many theoretical and experimental works have revealed CNTs to be stiff, strong, and highly flexible nanoscale fibers, with a tensile modulus and individual nanotube strength of up to 1 TPa and 63 GPa, respectively, which surpasses all existing materials [13]. Other applications in electrochemical products, filter, biosensors, structural fibers, actuators, ultrafast photonics, and so forth have also been demonstrated [14–16]. However, the direct use of such nanoscaled structures in IC is still facing challenges because as-prepared CNTs have nonuniform and uncontrollable structures (diameter and chirality) that yield variation in their electronic properties [17]. Instead of pursuing chirality-pure and defect-free CNTs [18, 19], an alternative approach is to use macroscopic CNT assemblies with controlled orientation and configurations, such as 1D CNT fiber/bundle, 2D CNT film/sheet, 2D/3D CNT network, and 3D aligned CNT arrays or foams, directly or through simple postprocess treatment. For example, owing to their high specific surface area, vertically aligned CNT arrays are used as electrodes in sensors and supercapacitors [20]. Bucky papers have demonstrated relatively high electrical and thermal conductivity [21, 22]. High strength CNT fibers have been spun from vertically aligned CNT arrays [23, 24]. These macroarchitectures, depending on the manner in which they are assembled, display a variety of fascinating features that cannot be achieved using conventional materials.

Upon careful design, the unique properties of CNTs, for example, high mechanical strength and good electrical and

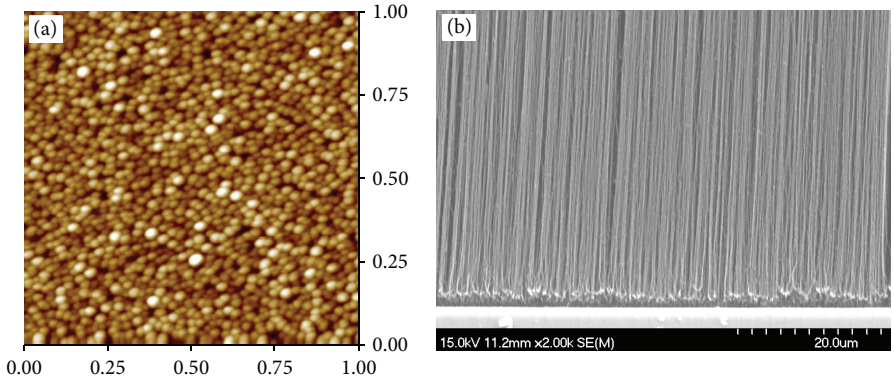

Figure 1: Morphology study of catalyst and CNT array. (a) AFM image ($1 \times 1\,\mu$m) of catalyst nanoparticles; (b) SEM image of spinnable CNT arrays.

thermal conductivity, can be retained in their macroscopic assemblies, enabling their potential applications in interconnection [25], thermal management [26], flexible electronics [27], touch display [28], and actuator and sensor [29, 30]. Among various macroscopic assemblies, well-aligned CNT bundle, CNT film, and CNT fibers are of particular interest because they can largely preserve the unique properties of individual CNTs and enable new advanced applications that existing materials cannot achieve.

In this paper, we report simple fabrication processes to produce CNT bundle, CNT fiber, and anisotropic CNT film from the same starting material: spinnable CNT array. We first synthesized vertical-aligned CNT arrays using a CVD method. The CNT bundle, CNT fiber, and CNT film are then obtained from such arrays through processes of direct peeling off, mechanical pressing, and pulling and twisting, respectively. The structures and properties of these assemblies have been extensively studied.

2. Materials and Methods

2.1. Synthesis of Spinnable 3D CNT Arrays. Vertically aligned CNT arrays were synthesized by a chemical vapor deposition method which is similar as we reported previously [7]. During the CNT growth, pure acetylene (C_2H_4) was used as the carbon source, and the forming gas, argon (Ar) and hydrogen (H_2), served as the carrier gas. Firstly we used a sputter to prepare catalyst, which is composed of a layer of Fe film and a supporting buffer layer of Al_2O_3 on a Si substrate. The thickness of the films was controlled by the sputtering time and the sputtering rate calibrated from thick films. In this study, optimal thickness of Fe layer is 1 nm and that of Al_2O_3 layer is 30 nm. Based on our previous study [31] that catalytic films must be cracked into small nanoparticles to promote CNT growth, the catalyst was then placed in the CVD furnace (Kejing, E0224-OTF-1200X) and annealed for 7 min at 750°C in a hydrogen environment, to reduce them into metallic state and break them into particles simultaneously. SEM (Jeol, JSM-7600F) was used to verify the morphology and uniformity of the CNTs in the as-grown vertically aligned CNT arrays. AFM (Asylum Research, Cypher AFM) was used to obtain the distribution of the catalyst after annealing. TEM (JEOL 2010) was used to identify the size and quality of individual CNTs. Figure 1(a) is a typical atomic-force-microscopy (AFM, Digital Instrument, S3000) image of such annealed catalyst, showing uniformly distributed catalyst nanoparticles with an average particle size of ~10 nm. Using such catalyst, the growth process was carried out for 10 min in CVD using argon as the carrier gas and ethylene as the carbon source. The as-grown CNT array was firstly checked by scanning electron microscopy (SEM). As shown in Figure 1(b), the vertically aligned CNT arrays with a controllable height in the range of 300–800 μm (depend on the carbon concentration and growth time) were successfully prepared. The SEM and Raman analysis confirmed the uniform and superaligned morphology. Transmission electron microscopy (TEM) measurements indicate these individual CNTs in the array are multiwalled nanotube (MWNT) with an average diameter of 6~7 nm and wall number of 3~4. We attribute high purity of the as-grown CNT arrays to the short growth time and high catalyst efficiency.

In order to fabricate CNT assemblies (bundle, film, and fiber) successfully, the as-synthesized CNT arrays must be spinnable. According to the previous studies, the spinning capability of a CNT array depends on top/bottom entanglement morphology [22], van der Waals interaction between the CNTs [32], and CNT height [33]. Zhang et al. [22] emphasized bundling within vertically grown CNTs and the disordered regions on the top and bottom of the arrays; these disordered regions help to preserve fiber integrity by interlocking the nanotubes. Studies reported by Li et al. [33, 34] found that highly aligned and clean (free of amorphous C) CNTs are critical for successful solid-state spinning. Experimentally, we have found that the spinning capability of CNT arrays could be optimized by controlling the catalyst state and the growth process. Effective catalyst state is the basic requirement for growing spinnable CNT arrays. Only those catalysts with small particle size, high density, and narrow size distribution can result in spinnable CNT arrays. CVD optimization was focused on the control of morphology, height, density, and uniformity of the arrays. Under optimal conditions, our spinnable CNT arrays possess

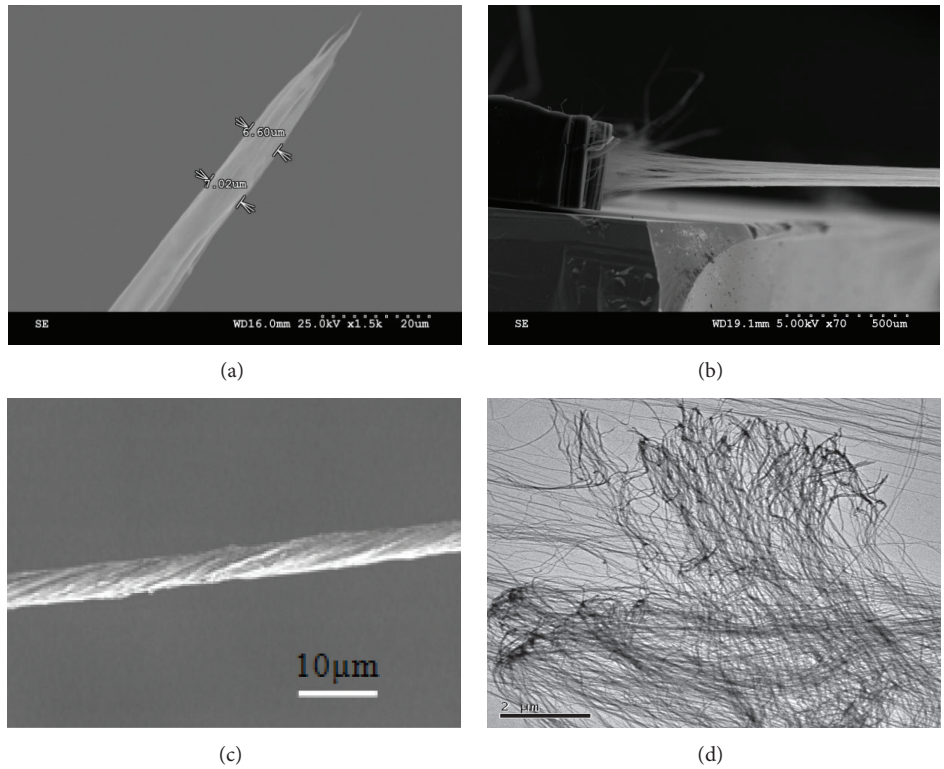

(a) (b)

(c) (d)

Figure 2: Fabrication of CNT bundles and CNT fibers. (a) SEM image of a CNT bundle; (b) SEM image shows a CNT ribbon pulled out from a CNT array; (c) SEM image of a CNT fiber; (d) TEM image shows connections between CNT ends.

a mass density around 0.02 g/cm^3 and an interspacing of 10~20 nm between individual CNTs. More than 1 m long yarn/ribbons could be easily pulled out from such arrays.

2.2. Fabrication and Characterization of Macroscopic CNT Assemblies

1D CNT Bundles. With the same starting material (vertically aligned CNT array), three different kinds of CNT assemblies have been fabricated. CNT bundles can be directly peeled off from as-grown CNT arrays, followed by densification by dipping them into ethanol. Such CNT bundles, with a density of about 0.1~0.2 g/cm^3, can be well designed for interconnects where high current-density is required. The diameter could be easily controlled by varying the amount of CNTs during peeling. Figure 2(a) is a SEM image of a CNT bundle with a diameter of 6~7 μm.

1D CNT Fibers. As-synthesized CNT powders are generally tens of micrometers in length and highly entangled. This feature of random orientation of nanotubes at a macroscopic level greatly hampers their use in potential applications, particularly in the composite fields. To fully utilize the excellent axial properties of CNTs, it is justifiable to make CNT-based fiber materials in which nanotube fillers are well aligned along the fiber axis. By mimicking the process of drawing silk out of a cocoon, spinning of the continuous CNT fibers from free-standing, super-aligned CNT array is a versatile method to orient nanotubes along the fiber axis. In this paper, a dry spinning method was used for fabrication of CNT fibers. In this process, pulling, twisting, and densification are accomplished at the same time. Continuous CNT yarn/ribbon was firstly pulled out from an array (Figure 2(b)) and then passed through ethanol. By introducing twisting, wide ribbon was narrowed and then packed into dense CNT fibers, as shown in Figure 2(c). The diameter of the fibers could be controlled by the width of initial yarn/ribbon. The pulling speed must be constant along fixed axial direction to guarantee the uniformity of prepared CNT fibers. It is worth to mention that not all CNT arrays can be successfully assembled into long and strong fibers. Key points for successful processing are believed to be effective entanglement morphology and enough van der Waals interaction between the CNTs. We characterized individual nanotubes in our CNT arrays by detailed TEM observation, as shown in Figure 2(d); direct and effective connections between individual CNT ends could be found, which is believed to be one of the reasons for successful spinning.

2D CNT Films. For CNT films, the widely used method in previous studies is focused on postprocessing of dispersed CNTs, and the resultant films have randomly distributed/orientated CNTs. To fully utilize the highly anisotropic properties of CNTs, here we prepare highly ordered CNT films using a simple mechanical process. Different from the randomly oriented Bucky paper described above, a simple and effective method called "domino pushing" was proposed to fabricate

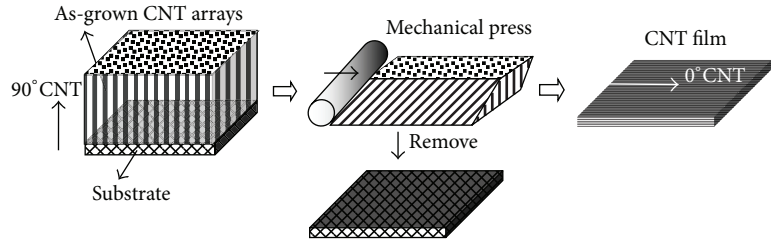

Figure 3: The fabrication process of CNT films.

aligned microthick CNT film using aligned MWNT arrays as a starting material. As shown in Figure 3, the as received MWNT arrays were forced down in one direction by pushing a cylinder with constant pressure, and thereby all nanotubes in the array were attracted together due to strong van der Waals forces and formed an aligned film or so-called Bucky paper. The aligned CNT film was then peeled off from substrate for characterization. In this way, vertically aligned CNT arrays could be transferred into unidirectional CNT films with good alignment and uniform structures. The area, thickness, and specific area of the CNT film is controllable by varying the substrate size, array length, and CNT site density. Our as-prepared CNT film possesses a thickness of around 10 μm, which can be directly used in the electrical devices (electrode, supercapacitors).

3. Properties of Macroscopic CNT Assemblies

3.1. Property of 1D CNT Bundles. Electrical properties of CNT bundles, CNT films, and CNT fibers were investigated and compared. Since the CNT bundles could be formed *in situ* on Si wafer, they are very attractive for through-wafer interconnection. Therefore their electrical conductivity is of our prime interest. A large number of CNT bundles with different diameters have been electrically tested, and the results are shown in Figure 4(a). As expected, the resistivity is reversely proportional to the cross-sectional area in a large range of CNT bundle size. The resistivity of the CNT bundles decreased gradually with increasing cross-sectional area of these bundles. From this tendency, we can extract an electrical resistivity of around $2\sim10 \times 10^{-4}$ Ω·m or a conductivity of 20~50 S/cm for our CNT bundles. It is necessary to mention that this kind of CNT bundles is directly prepared from as-grown CNT arrays without any posttreatment. Comparing to the conductivity of CNT fibers, this number is quite low and the possible reason could be due to the poor densification in bundle processing.

3.2. Property of 2D CNT Film. We fabricated CNT films into the size of 5 mm × 10 mm with a thickness of 10 μm for electrical testing. Since the film is structurally unidirectional, the electrical conductivities of the CNT films were then measured along both the 0° (parallel to CNT alignment) and 90° (perpendicular to CNT alignment) directions. A typical current-voltage (I-V) curve is shown in Figure 4(b), and the resistivity and conductivity are listed in Table 1.

Table 1: The electrical resistivity and conductivity of different CNT assemblies.

CNT assemblies	Electrical resistivity (Ω·m)	Conductivity (S/cm)
CNT bundle	$2\sim5 \times 10^{-4}$	20~50
CNT film 0°	$4\sim7 \times 10^{-5}$	145~250
CNT film 90°	$6\sim9 \times 10^{-5}$	110~150
CNT fiber	$2\sim5 \times 10^{-5}$	200~500

The I-V curve is linear, indicating the metallic feature of multiwalled CNTs. The electrical conductivity of the CNT films shows a slight difference in two testing directions, with a better conductivity of 145~250 S/cm along 0° direction (axial conductivity) and a slightly lower conductivity of 110~150 S/cm along 90° direction, whereas the value for conventional Bucky paper is 1.5 S/cm (aligned CNT films demonstrate two orders of magnitude). Such improvement is attributed to the fairly straight alignment of nanotubes. This indicates that the alignment of CNTs could be partially retained even after severe mechanical deformation. Further enhancement on the anisotropic structure/properties could be expected by introducing dragging force along alignment direction and/or reducing the thickness of the films.

Because of the high accessible surface area of porous nanotube morphology, in combination with their high electrical conductivity, low mass density, and chemical stability, the nontransparent CNT-based film/sheets are also attractive candidates for a variety of energy-conversion and storage technologies [35]. Examples include "supercapacitors," which give giant capacitances in comparison with those of ordinary dielectric-based capacitors. So far, driven by its promising high power density [36], CNT-based supercapacitors have not only achieved notable energy and power performances, they have also enabled new functionalities, providing flexible, stretchable, and transparent supercapacitors [37].

3.3. Property of 1D CNT Fiber. The electrical property of CNT fibers was also studied using a two-point probe. Similar linear I–V curves were obtained for each test of CNT fibers. Since the densification would affect the electrical properties of CNT assemblies (as in CNT bundles), the influence of twisting on fiber property was studied. We have investigated three types of CNT fibers with different twisting speeds but with the same drawing speed (15 mm/min): CNT fibers A, B, and C with twisting speed of 250 rpm, 200 rpm and 170 rpm, respectively.

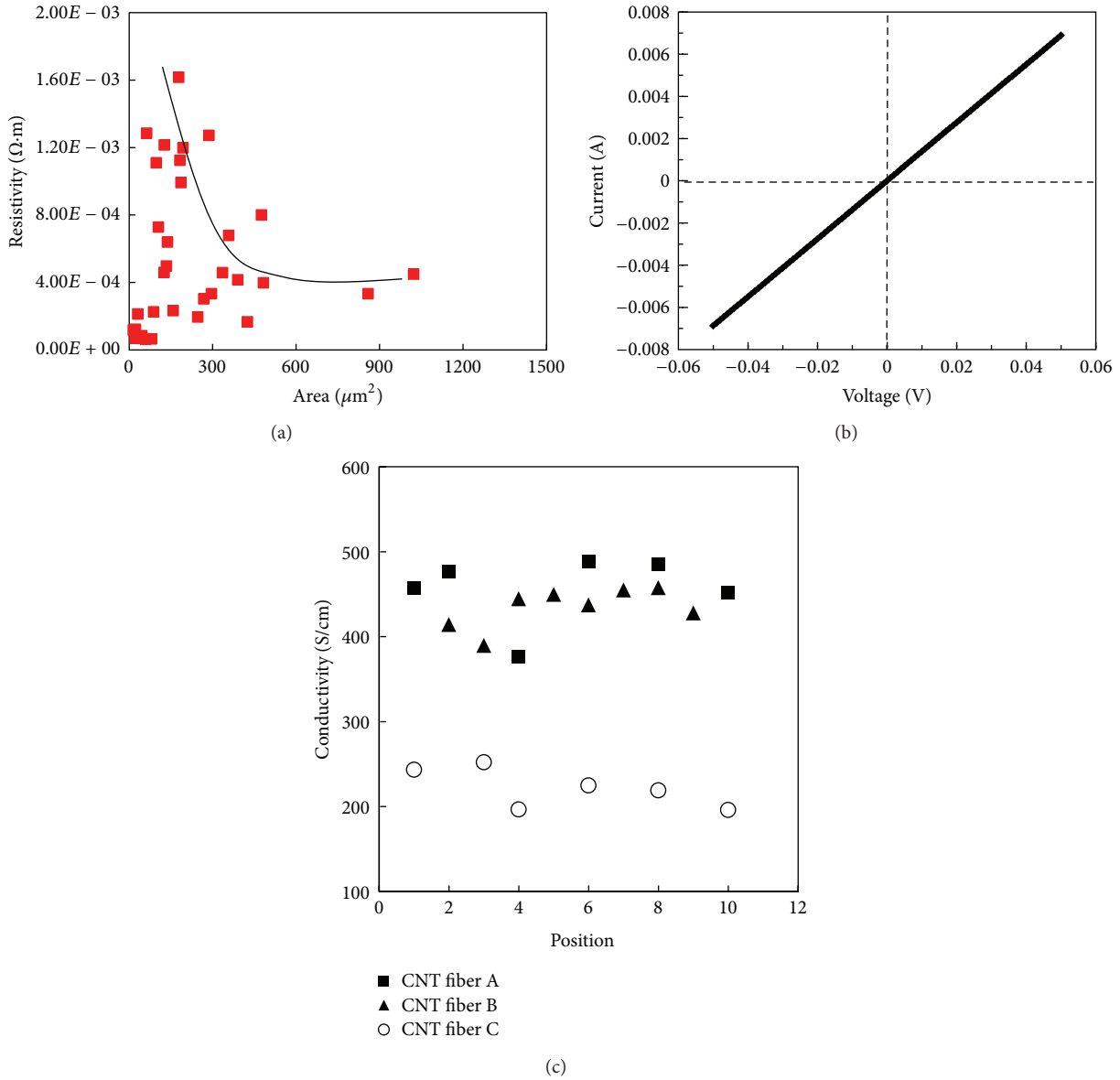

FIGURE 4: Electrical properties of CNT assemblies. (a) Resistance per length changes with cross-section area of CNT bundles; (b) typical I-V curve of CNT films; (c) electrical conductivity variation along the length and conductivity dependence on fiber twisting (CNT fiber A, fiber B, and fiber C are spun with the same drawing speed but with different twisting speed of 250 rpm, 200 rpm, and 170 rpm, resp.).

The electrical conductivity and its uniformity along the long fibers have been tested and the results are shown in Figure 4(c). Firstly, all fibers exhibit relatively stable conductivity (with ±10% variation around their average values) at different positions. And importantly, it is found that higher twisting speeds yield higher conductivity: the conductivity of CNT fiber A with 250 rpm twisting is about twice the conductivity of the fiber C which used 170 rpm twisting, indicating that effective twisting can result in a dense structure and introduce more interconnections between individual CNTs within the fibers.

For comparison, we summarized the electrical conductivities of three different CNT assemblies in Table 1. Since there is a wide range of the size variation in each type of samples, the data in the table is accordingly given as a range, instead of an average value, for each type of assembly. It is found that CNT fibers possess the best electrical conductivity (200~500 S/cm) while CNT bundles have the lowest conductivity (20~50 S/cm). The highest conductivity from CNT fibers is around 500 S/cm. This result is favorably comparable to the previous reported values of 300 S/cm and 400 S/cm for dry-drawn MWNT fibers [33] but is slightly lower than that of metal-coated CNT fibers [38]. Since the staring materials for three types of assemblies are exactly the same, the difference in conductivity must be attributed to the variation in physical structure which resulted from fabrication processes. We believe the packing density should be the dominate factor. Mechanical twisting together with liquid densification in

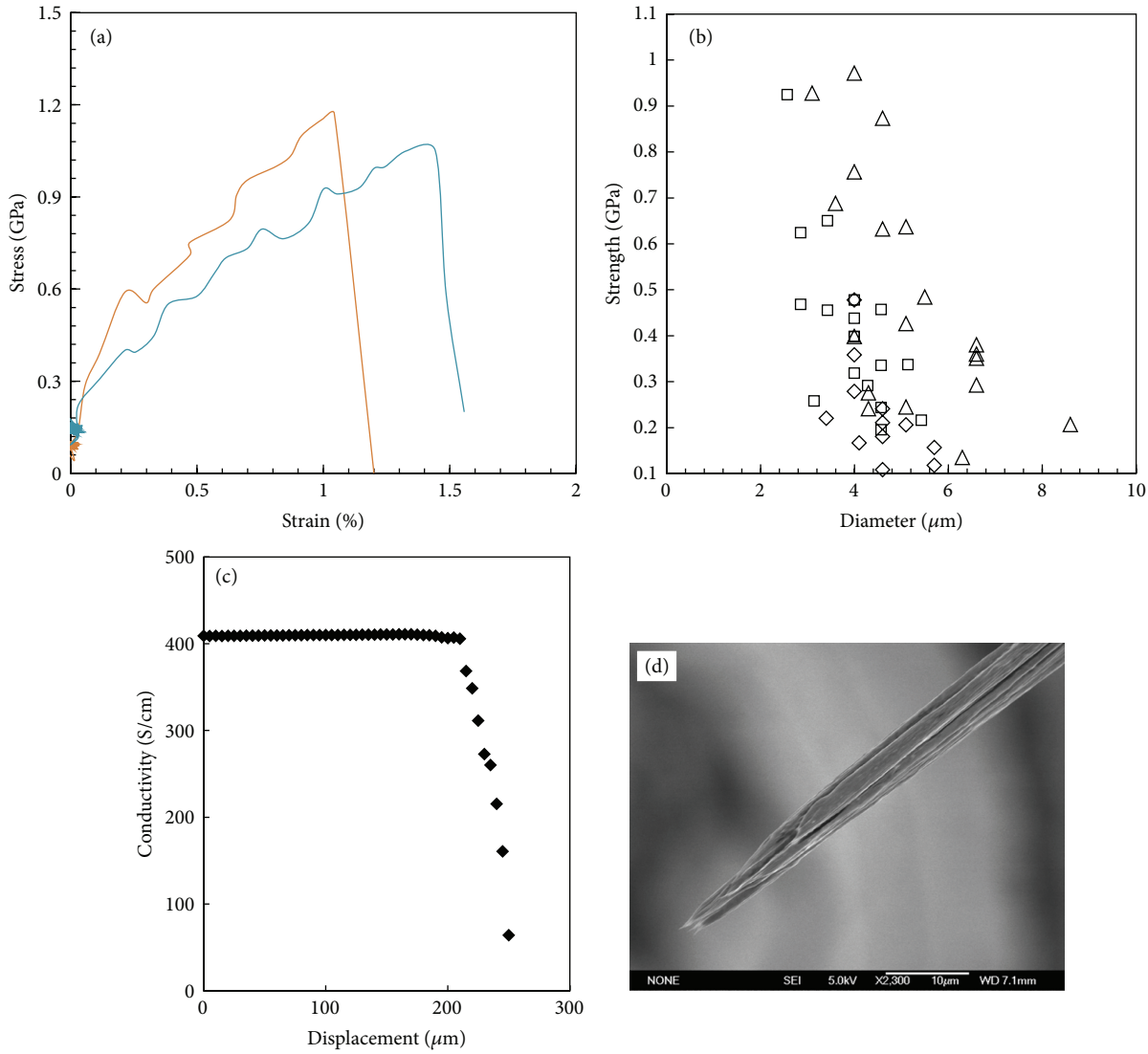

FIGURE 5: Mechanical properties of CNT fibers. (a) Tensile stress-strain curve of pure CNT fibers with a gauge length of 5 mm; (b) distribution of tensile strength versus diameter of CNT fibers; (c) the variation of electrical conductivity during stretching; (d) SEM image on fracture surface of CNT fiber.

fiber process can effectively put more CNTs into a compact structure and thus yield a high conductivity.

Due to their lightweight and good conductivity, CNT fibers are attractive to be used as conducting wires for aerospace or deep-sea oil drilling, or even the supporting cable of future space elevator. In these applications, mechanical property and/or conductivity under mechanical load are important. The mechanical tensile property of CNT fibers was then studied with a gauge length of 10 mm. They exhibit elastic smooth stress-strain curves: a linear relation with high modulus at small strain, followed by nonlinear relation and a decreased modulus. The tensile strength of these CNT fibers can reach up to ~1.2 GPa with a break strain around 2%. Yong's moduli of all tested fibers are statistically distributed in the range of 70–125 GPa. Figure 5(a) is the typical stress-strain curve of the CNT fibers; we found that all the curves include three stages: a typical linear stage at the beginning, a nonlinear stage with a lower slope in the middle, and a final failure stage. When further investigating the influence of the strain rate on mechanical response of CNT fibers, a strain rate strengthening effect of CNT fibers was obtained. A higher strain rate results in a high strength and a small fracture strain, while a lower strain rate produces a much larger fracture strain but a lower strength. The slope of stress-strain curve at the beginning of tension is also changed accordingly and shows higher Yong's moduli of the fibers under faster tensile conditions. For the final failure stage, it always shows brittle break at high strain rates, but both brittle break and ductile failure have been observed at low strain rates. More details about the influence of strain rate on mechanical behavior of pure CNT fibers can be found in our previous work [4, 39]. Considering the influence of spinning process, we have summarized their tensile strength according to their diameter, as shown in Figure 5(b). It is

found that the fiber strength decreases with the diameter, and the highest strength is obtained from fibers with the diameter of 3~5 μm. This can be explained by the nonuniform twisting along the radial direction of the fibers. It is much easier to effectively transfer the twisting to the core part for small diameter fibers. But in large diameter fibers, mechanical twisting may only affect the outlayer CNTs, making core part still loosely packed.

The electrical conductivity of the CNT fibers under mechanical stretching was also studied by *in situ* monitoring the conductivity change during stretching. Figure 5(c) shows the conductivity change according to tensile displacement (gauge length is 10 mm). When the mechanical tension is applied with a displacement less than 200 μm, the conductivity kept at the same level (~400 S/cm) without much decrease. Further stretching the CNT fiber above 200 μm will result in a significant decrease in conductivity. The stain at this point is about 2%, which is close to the break strain of our CNT fibers. We believe that, under the mechanical stretching of CNT fibers, there is always a critical stress point. Below such a critical stress, CNTs within the fibers may extend their length through strain building or CNT sliding, without the generation of permanent damage; however, the high stress above such a critical point may produce large amount of defects and form permanent damage (break CNT connection) in CNT fibers. Therefore, the conductivity decrease in CNT fibers should be related to the breaking-down process of CNT fibers. Figure 5(d) is a SEM image on fractured surface of the CNT fiber, which could be used to study the breaking mechanism of the CNT fibers. We have found that the CNT fiber loses its twisting structure after break and show a gradual fracture surface. Nevertheless, the results suggest that the electrical conductivity of our CNT fibers is stable under stretching before break, at least under our current testing conditions. Extensive testing under various conditions is still needed for practical wiring applications.

4. Conclusions

Macroscale CNT assemblies including CNT bundle, CNT film, and CNT fiber have been successfully fabricated from spinnable CNT arrays, and their electrical and mechanical properties have been studied. By optimizing the distribution and morphology of catalysts, uniform and top-entangled individual CNTs within a vertically 3D CNT array could be obtained to ensure good spinnability of CNTs. Since these macroscale CNT assemblies are fabricated from the vertically aligned CNT arrays, they can preserve much of the one-dimensional nature of individual CNTs and demonstrate their excellent electrical and also mechanical properties. CNT bundles show advantages in interconnect applications. Our 2D aligned CNT films demonstrated their electrical conductivity (145~250 S/cm) two orders of magnitude higher than conventional Bucky paper and showed their difference along 0° and 90° alignment of CNTs within film. The CNT fiber showed their high and uniform conductivity (about 400~500 S/cm) and excellent mechanical properties (1.2 GPa of tensile strength), and more importantly the stable electrical conductivity under stretching condition. Compared with nanoscale individual CNTs, these engineered macroscale CNT assemblies are easy to handle, design, and test. Together with the simple fabrication processes, these CNT assemblies may open a wide range application in advanced electronics.

Conflict of Interests

The authors declare that there is no conflict of interests regarding the publication of this paper.

Acknowledgments

This work was financially supported by Shaanxi Province Foundation for Fundamental Research and NPU Foundation for Fundamental Research (no. NPU96-QZ-2014, no. 3102014JCQ01031, and no. 2014JQ6229) in China.

References

[1] R. H. Baughman, A. A. Zakhidov, and W. A. de Heer, "Carbon nanotubes—the route toward applications," *Science*, vol. 297, no. 5582, pp. 787–792, 2002.

[2] J. Appenzeller, R. Martel, V. Derycke et al., "Carbon nanotubes as potential building blocks for future nanoelectronics," *Microelectronic Engineering*, vol. 64, no. 1–4, pp. 391–397, 2002.

[3] Y. N. Zhang and L. X. Zheng, "Towards chirality-pure carbon nanotubes," *Nanoscale*, vol. 2, no. 10, pp. 1919–1929, 2010.

[4] Y. N. Zhang, L. X. Zheng, G. Z. Sun, Z. Y. Zhan, and K. Liao, "Failure mechanisms of carbon nanotube fibers under different strain rates," *Carbon*, vol. 50, no. 8, pp. 2887–2893, 2012.

[5] G. Z. Sun, J. Q. Liu, L. X. Zheng, W. Huang, and H. Zhang, "Preparation of weavable, all-carbon fibers for non-volatile memory devices," *Angewandte Chemie—International Edition*, vol. 52, no. 50, pp. 13351–13355, 2013.

[6] G. Z. Sun, L. X. Zheng, J. N. An et al., "Clothing polymer fibers with well-aligned and high-aspect ratio carbon nanotubes," *Nanoscale*, vol. 5, no. 7, pp. 2870–2874, 2013.

[7] L. X. Zheng, G. Z. Sun, and Z. Y. Zhan, "Tuning array morphology for high-strength carbon-nanotube fibers," *Small*, vol. 6, no. 1, pp. 132–137, 2010.

[8] M. Radosavljević, J. Lefebvre, and A. T. Johnson, "High-field electrical transport and breakdown in bundles of single-wall carbon nanotubes," *Physical Review B—Condensed Matter and Materials Physics*, vol. 64, no. 24, Article ID 241307, 2001.

[9] P. G. Collins, M. S. Arnold, and P. Avouris, "Engineering carbon nanotubes and nanotube circuits using electrical breakdown," *Science*, vol. 292, no. 5517, pp. 706–709, 2001.

[10] A. Javey, R. Tu, D. B. Farmer, J. Guo, R. G. Gordon, and H. Dai, "High performance n-type carbon nanotube field-effect transistors with chemically doped contacts," *Nano Letters*, vol. 5, no. 2, pp. 345–348, 2005.

[11] Z. Chen, J. Appenzeller, Y.-M. Lin et al., "An integrated logic circuit assembled on a single carbon nanotube," *Science*, vol. 311, no. 5768, p. 1735, 2006.

[12] A. Bachtold, P. Hadley, T. Nakanishi, and C. Dekker, "Logic circuits with carbon nanotube transistors," *Science*, vol. 294, no. 5545, pp. 1317–1320, 2001.

[13] M.-F. Yu, O. Lourie, M. J. Dyer, K. Moloni, T. F. Kelly, and R. S. Ruoff, "Strength and breaking mechanism of multiwalled

carbon nanotubes under tensile load," *Science*, vol. 287, no. 5453, pp. 637–640, 2000.

[14] M. L. Yola and N. Atar, "A novel voltammetric sensor based on gold nanoparticles involved in p-aminothiophenol functionalized multi-walled carbon nanotubes: application to the simultaneous determination of quercetin and rutin," *Electrochimica Acta*, vol. 119, pp. 24–31, 2014.

[15] H. Karimi-Maleh, P. Biparva, and M. Hatami, "A novel modified carbon paste electrode based on NiO/CNTs nanocomposite and (9, 10-dihydro-9, 10-ethanoanthracene-11, 12-dicarboximido)-4-ethylbenzene-1, 2-diol as a mediator for simultaneous determination of cysteamine, nicotinamide adenine dinucleotide and folic acid," *Biosensors and Bioelectronics*, vol. 48, pp. 270–275, 2013.

[16] B. J. Sanghavi and A. K. Srivastava, "Simultaneous voltammetric determination of acetaminophen, aspirin and caffeine using an in situ surfactant-modified multiwalled carbon nanotube paste electrode," *Electrochimica Acta*, vol. 55, no. 28, pp. 8638–8648, 2010.

[17] S. M. Bachilo, M. S. Strano, C. Kittrell, R. H. Hauge, R. E. Smalley, and R. B. Weisman, "Structure-assigned optical spectra of single-walled carbon nanotubes," *Science*, vol. 298, no. 5602, pp. 2361–2366, 2002.

[18] L. X. Zheng, M. J. O'Connell, S. K. Doorn et al., "Ultralong single-wall carbon nanotubes," *Nature Materials*, vol. 3, no. 10, pp. 673–676, 2004.

[19] L. X. Zheng, B. C. Satishkumar, P. Q. Gao, and Q. Zhang, "Kinetics studies of ultralong single-walled carbon nanotubes," *Journal of Physical Chemistry C*, vol. 113, no. 25, pp. 10896–10900, 2009.

[20] G. Z. Sun, Y. X. Huang, L. X. Zheng et al., "Ultra-sensitive and wide-dynamic-range sensors based on dense arrays of carbon nanotube tips," *Nanoscale*, vol. 3, no. 11, pp. 4854–4858, 2011.

[21] X. F. Zhang, T. V. Sreekumar, T. Liu, and S. Kumar, "Properties and structure of nitric acid oxidized single wall carbon nanotube films," *The Journal of Physical Chemistry B*, vol. 108, no. 42, pp. 16435–16440, 2004.

[22] M. Zhang, S. Fang, A. A. Zakhidov et al., "Materials science: strong, transparent, multifunctional, carbon nanotube sheets," *Science*, vol. 309, no. 5738, pp. 1215–1219, 2005.

[23] X. F. Zhang, Q. W. Li, T. G. Holesinger et al., "Ultrastrong, stiff, and lightweight carbon-nanotube fibers," *Advanced Materials*, vol. 19, no. 23, pp. 4198–4201, 2007.

[24] L. X. Zheng, X. F. Zhang, Q. W. Li et al., "Carbon-nanotube cotton for large-scale fibers," *Advanced Materials*, vol. 19, no. 18, pp. 2567–2570, 2007.

[25] J. Li, Q. Ye, A. Cassell et al., "Electronic properties of multiwalled carbon nanotubes in an embedded vertical array," *Applied Physics Letters*, vol. 81, no. 5, pp. 910–912, 2002.

[26] M. J. Biercuk, M. C. Llaguno, M. Radosavljevic, J. K. Hyun, A. T. Johnson, and J. E. Fischer, "Carbon nanotube composites for thermal management," *Applied Physics Letters*, vol. 80, no. 15, pp. 2767–2769, 2002.

[27] E. Artukovic, M. Kaempgen, D. S. Hecht, S. Roth, and G. Grüner, "Transparent and flexible carbon nanotube transistors," *Nano Letters*, vol. 5, no. 4, pp. 757–760, 2005.

[28] S. L. Hellstrom, H. W. Lee, and Z. N. Bao, "Polymer-assisted direct deposition of uniform carbon nanotube bundle networks for high performance transparent electrodes," *ACS Nano*, vol. 3, no. 6, pp. 1423–1430, 2009.

[29] R. H. Baughman, C. X. Cui, A. A. Zakhidov et al., "Carbon nanotube actuators," *Science*, vol. 284, no. 5418, pp. 1340–1344, 1999.

[30] A. Modi, N. Koratkar, E. Lass, B. Wei, and P. M. Ajayan, "Miniaturized gas ionization sensors using carbon nanotubes," *Nature*, vol. 424, no. 6945, pp. 171–174, 2003.

[31] Z.-Y. Zhan, Y.-N. Zhang, G.-Z. Sun, L.-X. Zheng, and K. Liao, "The effects of catalyst treatment on fast growth of millimeter-long multi-walled carbon nanotube arrays," *Applied Surface Science*, vol. 257, no. 17, pp. 7704–7708, 2011.

[32] X. B. Zhang, K. L. Jiang, C. Feng et al., "Spinning and processing continuous yarns from 4-inch wafer scale super-aligned carbon nanotube arrays," *Advanced Materials*, vol. 18, no. 12, pp. 1505–1510, 2006.

[33] X. F. Zhang, Q. W. Li, Y. Tu et al., "Strong carbon-nanotube fibers spun from long carbon-nanotube arrays," *Small*, vol. 3, no. 2, pp. 244–248, 2007.

[34] Q. W. Li, X. F. Zhang, R. F. DePaula et al., "Sustained growth of ultralong carbon nanotube arrays for fiber spinning," *Advanced Materials*, vol. 18, no. 23, pp. 3160–3163, 2006.

[35] L. Hu, M. Pasta, F. La Mantia et al., "Stretchable, porous, and conductive energy textiles," *Nano Letters*, vol. 10, no. 2, pp. 708–714, 2010.

[36] V. L. Pushparaj, M. M. Shaijumon, A. Kumar et al., "Flexible energy storage devices based on nanocomposite paper," *Proceedings of the National Academy of Sciences of the United States of America*, vol. 104, no. 34, pp. 13574–13577, 2007.

[37] P.-C. Chen, G. Shen, S. Sukcharoenchoke, and C. Zhou, "Flexible and transparent supercapacitor based on In_2O_3 nanowire/carbon nanotube heterogeneous films," *Applied Physics Letters*, vol. 94, no. 4, Article ID 043113, 2009.

[38] Q. W. Li, Y. Li, X. F. Zhang et al., "Structure-dependent electrical properties of carbon nanotube fibers," *Advanced Materials*, vol. 19, no. 20, pp. 3358–3363, 2007.

[39] G. Z. Sun, L. X. Zheng, J. Y. Zhou, Y. N. Zhang, Z. Y. Zhan, and J. H. L. Pang, "Load-transfer efficiency and mechanical reliability of carbon nanotube fibers under low strain rates," *International Journal of Plasticity*, vol. 40, pp. 56–64, 2013.